Biomaterials Science

Substrate-dependent regeneration capacity of mesenchymal stem cell spheroids derived on various biomaterial surfaces

Journal:	*Biomaterials Science*
Manuscript ID:	BM-ART-02-2014-000053.R2
Article Type:	Paper
Date Submitted by the Author:	15-May-2014
Complete List of Authors:	Huang, Guo-Shiang; National Taiwan University, Hsieh, Pai-Shan; National Taiwan University, Tseng, Ching-Shiow; National Central University, Hsu, Shan-hui; National Taiwan University,

Journal Name

RSCPublishing

ARTICLE

Substrate-dependent regeneration capacity of mesenchymal stem cell spheroids derived on various biomaterial surfaces

Cite this: DOI: 10.1039/x0xx00000x

Received 00th January 2012,
Accepted 00th January 2012

DOI: 10.1039/x0xx00000x

www.rsc.org/

Guo-Shiang Huang[a, #], Pai-Shan Hsieh[a, #], Ching-Shiow Tseng [b], Shan-hui Hsu [a, *]

Mesenchymal stem cells (MSCs) are widely used for their self-renewal and multipotent abilities, which can be further enhanced by growing MSCs as three-dimensional (3D) cellular spheroids on certain substrates. Although various surfaces have been used to generate 3D MSC spheroids, the answer to whether all these spheroids have similar in vitro and in vivo properties remains unclear. In this study, adipose-derived adult stem cells (ADSCs) were cultured on the non-adherent petri dish, polyvinyl alcohol, chitosan (CS), or chitosan-hyaluronan (CS-HA) to form 3D spheroids. The expression of cell adhesion molecule, N-cadherin, was analyzed by qRT-PCR and Western blotting. Functional migration ability was tested using the transwell assay. The capacity for chondral regeneration of various ADSC spheroids were further evaluated in a rabbit model. We demonstrated that ADSC spheroids derived on CS or CS-HA surface had the greater expression of N-cadherin and better migration ability. The latter was consistent with the higher expression levels of chemokine/receptor SDF-1/CXCR4 for the spheroids derived on CS or CS-HA. Animal studies also revealed significantly better cartilage repair in defects loaded with CS- or CS-HA-derived spheroids. In particular, CS-HA-derived spheroids gave rise to the best regeneration when combined with a 3D printed scaffold. This study suggested that MSC spheroids derived on different surfaces may have distinct in vitro and in vivo properties, which appeared to be associated with the surface-bound calcium as well as the calcium-dependent N-cadherin and CXCR4 signalings. The substrate-dependent properties may eventually lead to the different regeneration capacity of various MSC spheroids in vivo.

Introduction

Adipose-derived adult stem cells (ADSCs) are one type of widely used mesenchymal stem cells (MSCs), which are capable of self-renewal and multilineage differentiation[1]. Compared to MSCs derived from bone marrow, a gold standard of MSCs, ADSCs are more accessible by a minimally invasive procedure with a sufficient number of cells[2]. Studies have demonstrated that ADSCs are multipotent and can undergo adipogenesis, osteogenesis, and chondrogenesis[3]. These characters make ADSCs a popular type of MSCs for research in tissue engineering and regenerative medicine. Autologous chondrocytes, being a cell source for cartilage tissue engineering, may be limited by the donor site availability (e.g. the non-weight-bearing area of the cartilage). It may take a longer period for expanding chondrocytes because of the low cell number and activity. MSCs which possess the chondrogenic capacity are an excellent alternative for the cell source. The autologous ADSCs can prevent the patients from the immune rejection of transplanted cells. The culture of ADSCs does not seem to result in tumor formation after transplantation[4]. Moreover, ADSCs have been used in human clinical trials[5].

MSCs are sensitive to their microenvironment, which strongly influences their behavior[6]. Three-dimensional (3D) culture resembles physiological conditions and is considered advantageous for keeping cellular functions[7]. 3D culture environment can be offered by biomaterials such as hydrogels and scaffolds, or by forming cell aggregates[7-9]. Forming 3D cell aggregates by the conventional hanging drop method has been suggested as a means to enhance the therapeutic potential and anti-inflammatory effects of MSCs[10,11]. Culture of MSCs on non-adherent dish or substrates such as polyvinyl alcohol

(PVA) also yielded viable MSC spheroids[12-14]. Moreover, MSCs attached on chitosan were able to self-assemble and form spheroids within two days. These self-assembled MSC spheroids showed greater stemness and differentiation capabilities[15].

Culture of MSCs as cell aggregates by pellet culture technique has been long used for increasing the chondrogenic potential in vitro[16,17]. Other methods such as hanging drop or self-assembly caused a similarly positive effect on MSC chondrogenesis[10, 18]. Recent reports have demonstrated that the use of MSC spheroids formed by hanging drop and suspension culture could enhance their therapeutic potential for cartilage regeneration in vivo[19,20].

During spheroid formation, several molecules related to cell adhesion and cell migration were involved, e.g. N-cadherin[21]. The expression level of N-cadherin was upregulated during spheroid formation, which was associated with the capacity for self-renewal and multilineage differentiation[22]. The stromal cell-derived factor-1 (SDF-1) is an essential chemokine for homing and migration of MSCs[23,24]. The signaling transduction by SDF-1 binding to chemokine (C-X-C motif) receptor type 4 (CXCR4) was reported to be important in regulating the chondrogenesis in vitro[25]. Homing of MSCs by SDF-1 was shown to significantly enhance the chondrogenesis in vitro[26, 27].

Although different in vitro properties has been demonstrated between self-assembled spheroids and the spheroids made from hanging drop or non-adherent petri dish[22], it remains unclear if the self-assembled MSC spheroids are superior to other MSC spheroids in vivo. Here we transplanted dispersed MSC single cells or MSC spheroids generated by various methods into the rabbit articular cartilage defect model to investigate the possible differences in the therapeutic effect in vivo. We also proposed mechanisms that accounted for the different in vivo performances of these MSC spheroids.

Results

ADSCs obtained from the subcutaneous adipose tissue were subject to flow cytometry and qRT-PCR for surface markers and stemness gene expression, respectively. ADSCs were positive for markers of MSCs, including CD73, CD90, and CD105, while markers of endothelial cells and hematopoietic cells, CD31 and CD34, were few to absent (Fig. S1A in Electronic Supplementary Information (ESI)). Expression of Oct4, Sox2, and Nanog by ADSCs was all at a high level (Fig. S1B in ESI). These characteristics were generally consistent with our previous results on human ADSCs[15], approving the genuinity of ADSCs. Spheroid formation occurred for ADSCs cultured on various membranes for 72 h (Fig. 1). Spheroids of different sizes or numbers were observed, and those on CS-HA were in general larger than others (Table S1).

Upregulation of CXCR4 and SDF-1 expression in CS-HA groups was observed after culture for 1 d and 3 d (Fig. 2A). Spheroids from CS-HA membranes expressed significantly higher CXCR4 and SDF-1 than all the other groups. To verify if the highly expressed CXCR4 and SDF-1 could influence the migration ability of neighboring cells, the migration assay using the transwell culture system was conducted (Fig. 2B). The chemotactic effect by SDF-1 was the most obvious in CS and CS-HA groups, which was consistent with the gene expression data. This effect was totally blocked when the SDF-1 antagonist, AMD3100, was added to the culture system, which suggested that cell migration may be driven by SDF-1.

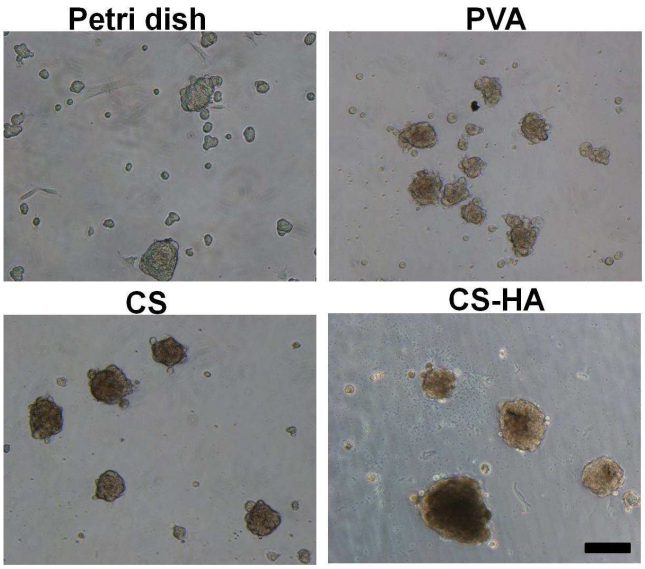

Fig. 1. Morphology of spheroids formed on various membranes. ADSCs were cultured on Petri dish, PVA, CS, and CS-HA. Spheroids were observed after 72 h by a phase contrast microscope. Scale bar: 100 μm.

The physical properties of the substrates are summarized in Table 1. There were differences in zeta potential and water contact angle among the substrates. However, these parameters seemed to have no correlation with the SDF-1 and CXCR4 expression. The concentration of the free (unbound) calcium and that of the surface bound calcium are shown in Fig. 3A. Both data indicated that CS and CS-HA bound significantly more calcium than the other substrates. Western blots of N-cadherin are demonstrated in Fig. 3B, from which the quantification was conducted. The expression level of N-cadherin was the highest in spheroids from CS-HA, followed by CS, low-adherent bacterial petri dish (Petri dish), PVA, and the dispersed single cells on tissue culture polystyrene (TCPS) (Fig. 3C). The N-cadherin expression of spheroids from CS was not much lower than that from CS-HA, whereas those from Petri dish and PVA were 50% less than that from CS-HA.

In addition to the difference in the expression of CXCR4, SDF-1, and N-cadherin, we also observed that the chondrogenic differentiation capacities in vitro were different for various spheroids (Fig. S2). The chondrogenic genes (Sox9, aggrecan, and collagen type II) were upregulated while the

collagen type I gene (fibrotic) and collagen type X gene (hypertrophic) were downregulated for spheroids on CS-HA and to a lesser extent on CS. Quantitative results of glycosaminoglycan (GAG) contents was consistent with the above findings, proposing that the chondrogenic differentiation potential was different among spheroids derived on various biomaterial substrates.

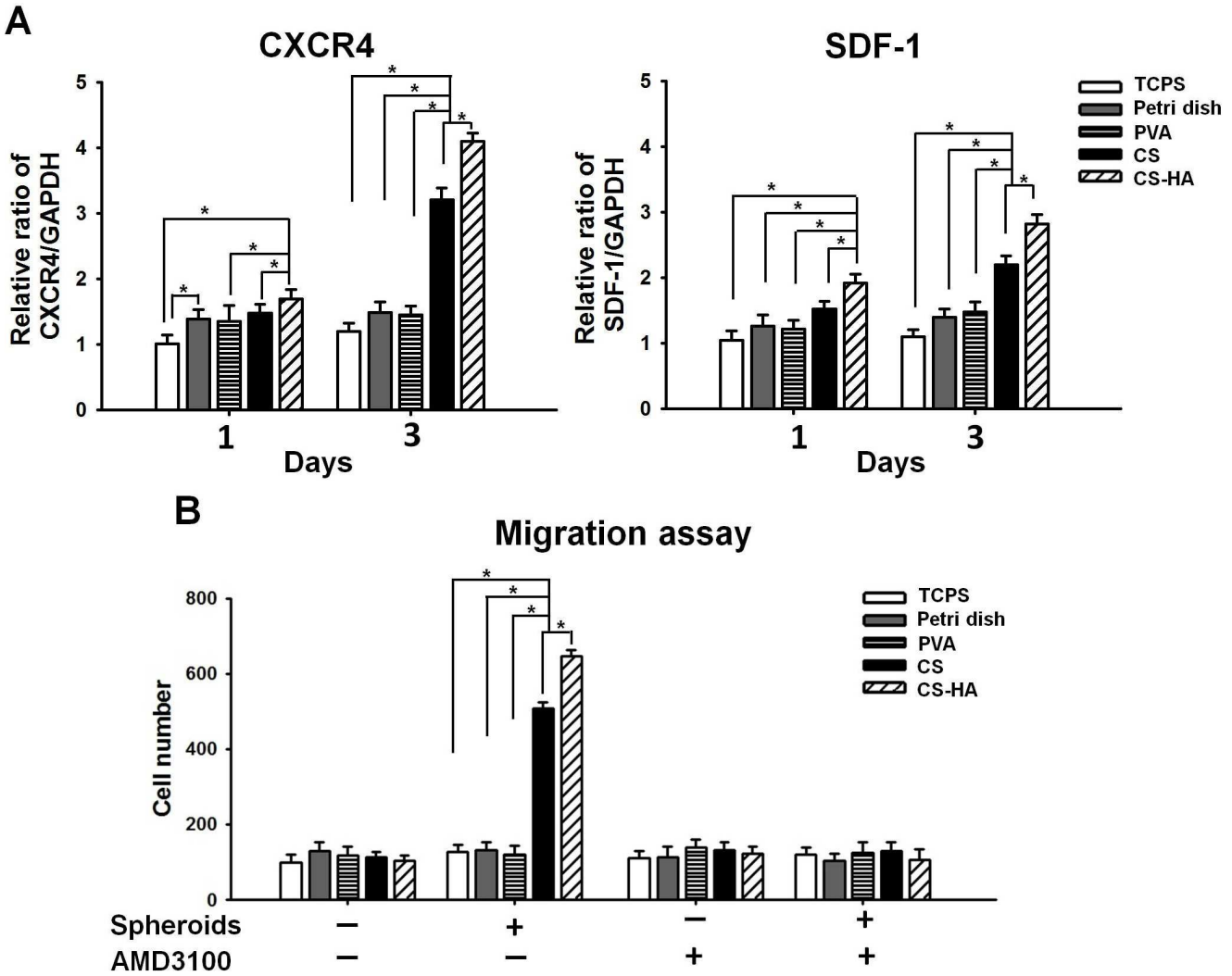

Fig. 2. Analysis of (A) CXCR4, SDF-1 expression and (B) migration ability of spheroids derived on various substrates. In the former test, ADSCs were cultured on various substrates for 1 and 3 days and collected for qRT-PCR of SDF-1. The gene expression was first expressed as the ratio to GAPDH (housekeeping gene) and all ratios were then normalized to the TCPS group at 1 day. In the latter test, the migration of ADSCs were evaluated by the transwell migration assay, in the absence or presence of AMD3100. TCPS indicates the control ADSC single cells cultured on TCPS. *p<0.05.

Table 1. The surface characterization of the materials.

Materials	Surface water contact angles (°)	Surface zeta potential (mV)
TCPS	65.0 ± 5.6	-19.0 ± 2.16
Petri dish	79.3 ± 2.8	-14.51 ± 1.28
PVA	51.3 ± 2.3	-16.2 ± 1.33
CS	83.8 ± 3.1	-3.51 ± 2.08
CS-HA	37.9 ± 4.2	-14.3 ± 1.86

From the histological staining of the animal studies, better regeneration was observed in CS and CS-HA groups than Petri dish, PVA, and TCPS (Fig. 4A), which had little red staining for GAG. Lacunae could be obviously found only in CS and CS-HA groups. Quantified intensity for GAG stain also showed the similar trend (Fig. 4B). The average stained area was the highest for CS-HA group and lowest for PVA, yet without significant difference (Fig. 4C). The ICRS histological score for regeneration demonstrated a significantly higher score for CS-HA compared to TCPS or

PVA (Fig. 4D). When combined with 3D printed scaffolds, the CS-HA spheroids had better regeneration effect than CS spheroids or dispersed single cells (TCPS)(Fig. 5A). Some pinkish white blocks could be found in the defect sites, which were the remains of the scaffolds that were not completely degraded. The quantified intensity of GAG for the CS-HA group was significantly higher than that for the groups of CS and TCPS (Fig. 5B). The stained area shown in Fig. 5C revealed a similar tendency. The histological score for the CS-HA group was also the highest, followed by CS and TCPS groups (Fig. 5D). Type II collagen was weakly stained in each group, and no tendency among groups could be clearly identified probably due to the relatively short recovery time (one month).

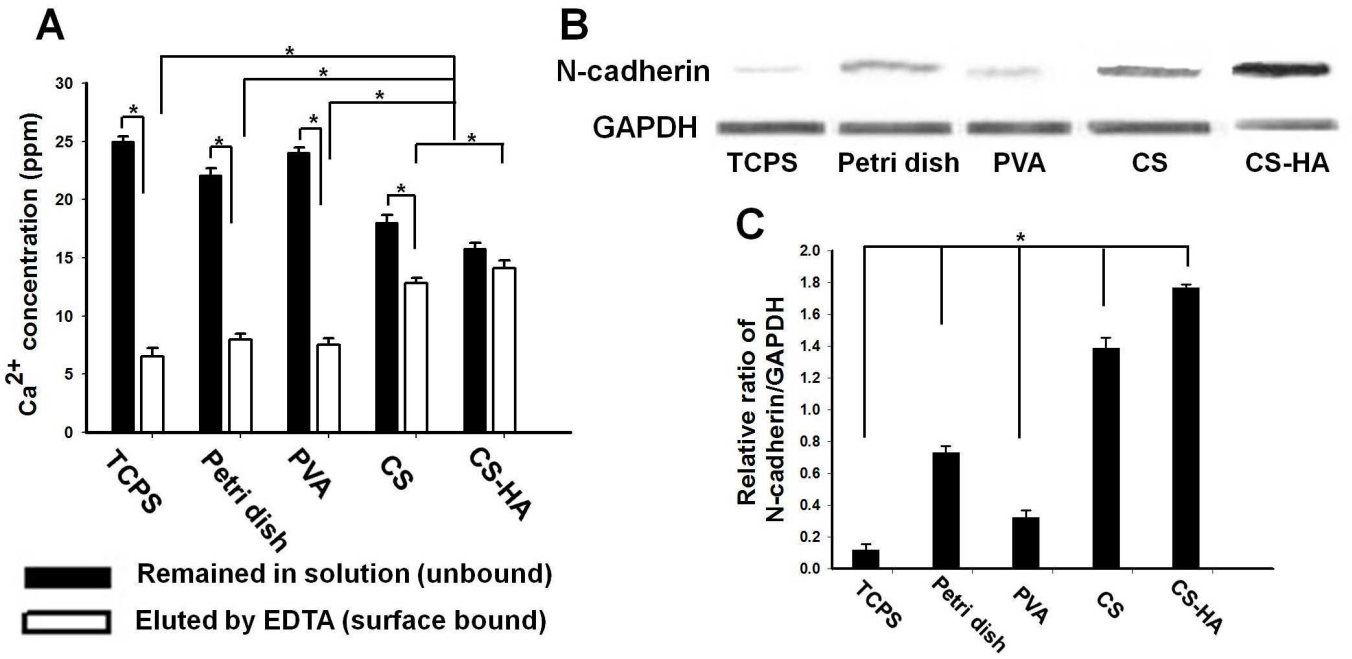

Fig. 3. Measurement of calcium content and protein expression of N-cadherin. (A) Quantification of amount of the free (unbound) calcium remained in the bulk solution and that of the surface bound calcium. (B) Western blotting of N-cadherin and the internal control GAPDH, and (C) semi-quantification of the N-cadherin expression levels for ADSCs cultured on various substrates for 72 h. *p<0.05.

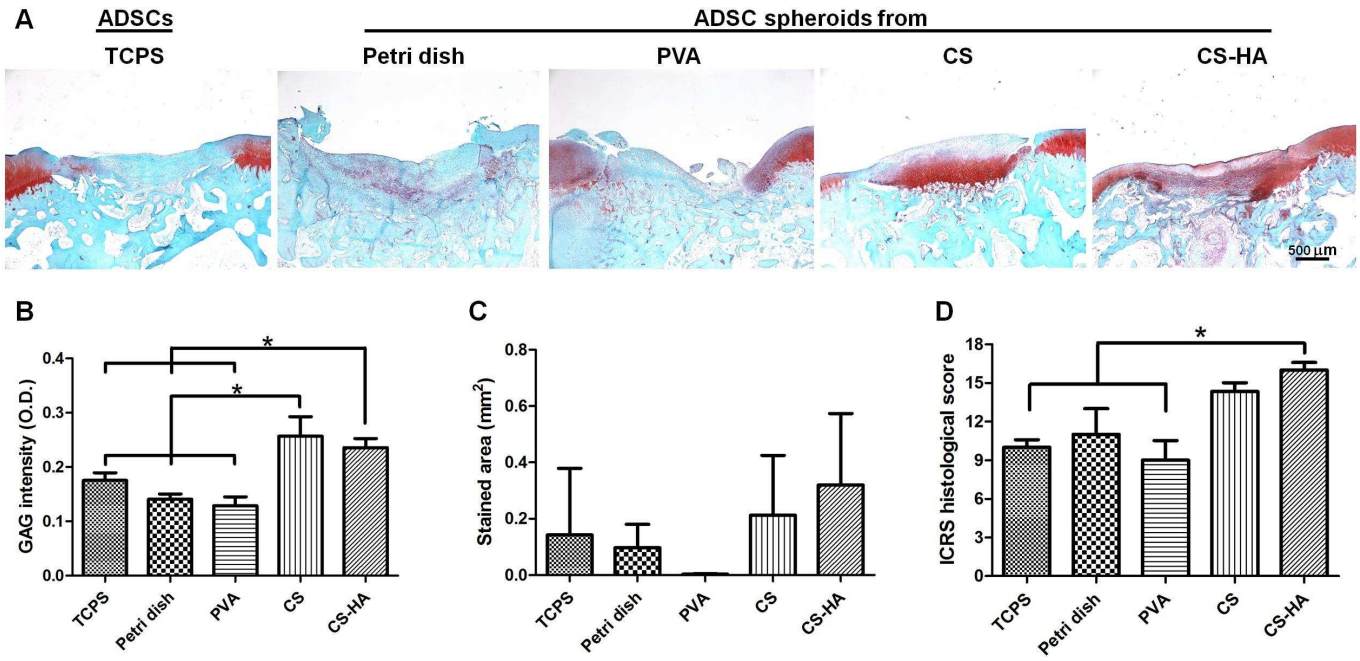

Fig. 4. Histological examination of defects receiving ADSC spheroids dervied on various substrates. TCPS indicates the control ADSC single cells cultured on TCPS. (A) Sections from animal implants (one month) were stained with Safranin O for glycosaminoglycan (GAG) expression. (B) The intensity of GAG stain and (C) the stained area quantified by image analysis. (D) The ICRS histological scores based on the sections. Scale bar: 500 μm. *p<0.05.

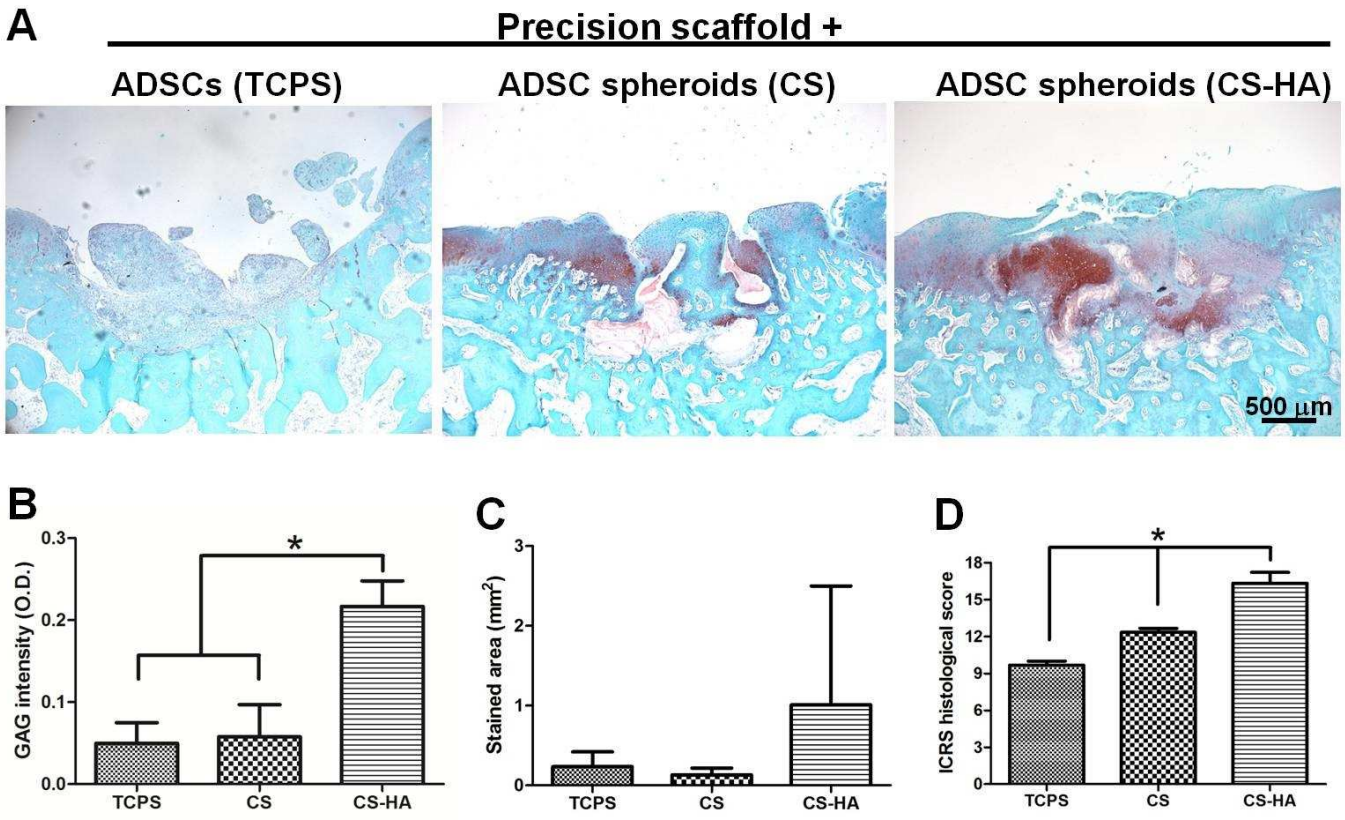

Fig. 5. Histological examination of defects receiving 3D printed scaffolds seeded with ADSC single cells, or spheroids derived on CS or CS-HA (one month). (A) Sections from animal implants were stained with Safranin O for GAG expression. (B) The intensity of GAG stain and (C) the stained area quantified by image analysis. (D) The ICRS histological scores based on the sections. Scale bar: 500 μm. *p<0.05.

Discussion

As a promising cell source for cell-based therapies, multipotent MSCs were advantageous in repairing or regenerating various tissues. Scientists have adjusted different parameters, such as the ingredients of culture medium, cell density, and various ways of culture, trying to enhance the differentiation capacity of MSCs. One way of the culture methods was to grow MSCs as cell aggregates or spheroids on different low-adherent substrates. In this study, we compared spheroids formed on several currently used substrates, and demonstrated the substrate-dependent properties in vitro and in vivo.

SDF-1 is a chemokine accounting for the homing effect of stem cells, and is highly associated with cell migration. Studies have shown that the elevation of local SDF-1 level caused the recruitment of circulating MSCs to the injured sites, and eventually improved the regeneration of the damaged tissue[28]. In this study, Spheroids on CS-HA expressed the most SDF-1 in vitro, and the difference was much more remarkable at 3 days. The cell migration assay, showed the number of recruited MSCs was the greatest for CS-HA-derived spheroids, followed by CS-derived spheroids, while those in the other groups were close to the basal level. The tendency was consistent with that of the SDF-1 expression. These observations suggested that the highly expressed SDF-1 by MSC spheroids derived on CS-HA may functionally attract nearby MSCs. This effect was abolished by the SDF-1 antagonist AMD3100, which further supported that the greater recruitment effect of CS-HA-derived MSC spheroids may be associated with the secretion of chemokine SDF-1.

In addition to the significantly greater SDF-1 gene expression, spheroids derived on CS-HA or CS also expressed more N-cadherin. Although the spheroids derived on PVA or by Petri dish only showed similar SDF-1 expression as single MSCs, the N-cadherin expression was higher than that of single MSCs grown on TCPS. This suggested that more cell-cell interaction may have taken place in all spheroids rather than in monolayer single cells. A previous study observed that the highly expressed N-cadherin may be associated with the differentiation ability of MSC spheroids[29,30].

Although the average size of the spheroids was somewhat different among groups, the sizes for PVA-derived and CS-derived spheroids were rather similar. The significant difference in the properties of the spheroids thus seemed not to be associated with the individual sizes.

Recent studies comparing MSC single cells with spheroids in vivo have shown that defects filled with MSC spheroids or aggregates resulted in better regeneration than those with single cells[19,31]. In current study, results from the preliminary animal study demonstrated that defects loaded with CS- or CS-HA-derived MSC spheroids showed better regeneration after 1 month. This agreed with the in vitro results and indicated that the cell recruitment effect as well as higher N-cadherin expression of the spheroids may predict the regeneration effect in vivo. On the other hand, PVA-derived spheroids had similar or lower regeneration effect than spheroids derived on low-adherent dish or single cells, suggesting the importance of the substrate to generate MSC spheroids on regeneration capacities.

When cells or spheroids were directly used for animal studies, the cell/spheroid suspension retained in the defect pretty well probably because of the capillary force and the high viscosity of HA (used to seal the defect). Certainly, there could be cell loss, and therefore PLGA 3D printed scaffolds were used for further experiments. In all experiments involving scaffolds, cells or spheroids were mixed with HA before injection into the stacking fibers of the 3D printed scaffolds. HA was added to facilitate the seeding of cells/spheroids into the 3D printed scaffolds and it did not interfere with the experimental outcome[32]. When spheroids were combined with scaffolds, spheroids derived on CS-HA had better in vivo results than those derived on CS and the regular MSC single cells. It was noticed that the size of CS-HA-derived spheroids was generally larger (~90 μm) than that of CS-derived spheroids (<80 μm). The larger spheroids may have better retention in large pores, giving to their higher efficacy. Overall, scaffolds seemed to serve as a base for CS-HA-derived spheroids to anchor on, leading to better generation in vivo.

Finally, one month is too short for complete cartilage repair. The animal experiment presented here only serve as a pilot study to support the different chondrogenic capacities of various biomaterial-derived spheroids. In particular, we found that CS-HA spheroids combined with PLGA scaffolds had good outcome only after one month. However, the possibility of hypertrophic differentiation at a later stage could not be ignored. On the other hand, since in vitro data proposed the lower collagen I and X expressions for CS-HA spheroids, they may have extra advantages in preventing the fibrosis or hypertrophy of the regenerated cartilage, which deserves further investigations. When considering a clinical application, the potential drawbacks could be the time required for spheroid formation, which may increase the risk of cell contamination. Without scaffolds, spheroids may be lost from the site. Although the use of scaffolds helps retain spheroids in the defect site, the PLGA scaffolds are not yet satisfactory. A more flexible scaffold for easy processing and fitting as well as fixation into the defect should improve the outcome of the strategy. In addition, MSC spheroids are larger in size. 3D printed scaffolds with macroporosity were thus used for seeding spheroids in this study. On the other hand, a more conventional tissue engineering scaffold (e.g. freeze-dried or microporous sponges) may not have a pore size large enough to accommodate the spheroids easily. Spheroids may not be readily seeded in such a scaffold and may only stay on the periphery of the scaffold. Therefore, designing a better biomaterial scaffold to carry these spheroids is essential for implementing the spheroids on the existing cartilage tissue engineering strategies in the future.

Experimental

Cell isolation

All animal procedures followed the ethical guidelines of the experimental animals and were approved by the Institutional Animal Care and Use Committee. Rabbit ADSCs were obtained from subcutaneous adipose tissue of New Zealand white rabbits. Extracted adipose tissue was minced and treated with 200 U/mL type I collagenase (Sigma) in phosphate buffered saline (PBS) at 37°C for 1 h with gentle agitation. Collected cells by centrifugation were seeded in a flask with Dulbecco's modified eagle medium-low glucose (DMEM-LG)/F12 (1:1) (Gibco) containing 10% fetal bovine serum (FBS) (Gibco) and 10 mg/L penicillin-streptomycin at 37°C in a 5% CO_2 incubator. Before performing single cell or spheroid culture, the primary cells were cultured on standard TCPS flasks and expanded to reach a sufficient amount of cells. Trypsin was regularly used during expansion. Cells of passages 3-5 were used in this study.

Analysis for the ADSCs

The expression of surface markers was quantified by flow cytometry using anti-CD29, anti-CD31, anti-CD44, and anti-CD90 (BioLegend), anti-CD34, anti-CD45 (Santa Cruz Biotechnology), anti-CD73, and anti-CD105 (BD Biosciences) antibodies. Cells (5×10^5) were washed with PBS, resuspended in 100 μL PBS with monoclonal antibodies, and incubated for 30 min at 4°C. After two washes by PBA, the cells were resuspended in 500 μL PBS. Fluorescence analysis was performed with a flow cytometer (FACS Caliber, BD Biosciences). The non-specific binding of the fluorescein isothiocyanate (FITC) and phosphatidyl ethanolamine (PE) conjugates were determined in control samples using a mouse IgG1-FITC and IgG1-PE negative control (Serotec). The stemness marker genes (Oct4, Sox2, and Nanog) were analyzed by real-time or quantitative RT-PCR (qRT-PCR). The multilineage differentiation capacities were conducted to verify the genuineness of the MSCs.

Preparation of polymer membranes

Chitosan (CS) powder was obtained from Fluka (USA, molecular weight: 510 kDa, degree of deacetylation: 77%). Hyaluronan (sodium salt, HA) was obtained from SciVision Biotech (Kaohsiung, Taiwan, molecular weight: 2500 kDa). Polyvinyl alcohol (PVA) was obtained from Sigma-Aldrich (molecular weight: 70-100 kDa). 300 μL chitosan (in 1% acetic acid) were dropped on cleansed 15-mm diameter circular microscope slides, which were air dried overnight and then immersed in 0.5 NaOH for 10 min. CS-coated slides were ready for use after three washes by PBS. 300 μL HA (3 mg/mL in distilled water) were dropped on the CS-coated slides and air dried overnight. The HA-coated CS membranes on slides were placed in 24-well culture plate for further crosslinking. 150 μL of ethyl(dimethylaminopropyl) carbodiimide/N-hydroxysuccinimide (EDC/NHS) solution with a weight ratio of HA/EDC/NHS adjusted to 1:1.84:0.23 at pH 5.5 was added to each well and shaken continuously for 48 h at 4°C to crosslink HA on the surface. After that, the membranes were washed five times with PBS to remove the unbound HA and were later lyophilized. The density of HA on CS-HA was approximately 0.5 mg/cm^2 [15]. 300 μL PVA (0.5% in distilled water) were dropped on cleansed 15-mm diameter circular microscope slides, which were air dried overnight. The surface water contact angle was measured by a static contact angle analyzer (FTA-1000 B, First Ten Angstrom Company, USA) at 25°C and 70% relative humidity. The surface zeta potential was measured by a particle size and zeta potential analyzer (Delsa™ Nano, Beckman Coulter, USA) using laser light scattering and a flat solid cell.

Spheroid formation on various membranes

One slide per well was placed in 24-well culture plates. ADSCs at a density 5×10^4 cells/well were loaded on TCPS, Petri dish, PVA, CS, and CS-HA membranes. After culture for 72 h, ADSCs on TCPS were trypsinized and collected as the dispersed ADSC single cells. Various ADSC spheroids on Petri dish, PVA, CS, and CS-HA membranes were harvested by aspiration. The formation of spheroids was observed at 72 h by a phase contrast microscope. The protein expression of N-cadherin was analyzed by Western blots. The gene expression of CXCR4 and SDF-1 was analyzed by qRT-PCR. The function expression of SDF-1 was further confirmed by the migration assay.

qRT-PCR analysis of CXCR4 and SDF-1

Total RNA of cells was extracted by using the Trizol® reagent (Invitrogen) according to the manufacturer's instruction. cDNA synthesis and amplification via PCR were performed using the RevertAid First Strand cDNA Synthesis Kit (MBI Fermentas, St. Leon-Rot, Germany). The qRT-PCR reaction was conducted and detected in a Chromo 4 PTC200 Thermal Cycler (MJ Research, USA) using the DyNAmo Flash SYBR Green qPCR Kit (Finnzymes Oy, Espoo, Finland). The expression levels were analyzed and normalized to GAPDH (the housekeeping gene). Sequences of primers used were listed in Table 2.

Cell labeling

ADSCs were labeled with an orange-red fluorescent dye (PKH26 Red Fluorescence Cell Linker Kit, Sigma). Cells (a density of 1×10^7 cells/mL) were labeled by mixing with 2×10^{-6} M PKH26, which could stably incorporate into cell membrane with its long aliphatic tails. The labeling process was stopped with complete medium. The labeled cells were washed and ready for use.

Cell migration assay

MSC spheroids (containing ~1×10^6 MSCs) were harvested at 72 h from each type of membranes and replated in the lower chamber of a transwell (fit in a 24 well plate) containing various membranes. The control groups were blank wells (TCPS) replated with 5×10^4 MSC single cells and those wells without any replated spheroids. Cells in the lower chamber were incubated for 3 days. 1×10^4 MSCs (PKH26 labeled) were further added to the upper chamber. After another 24 h, the upper surface of the transwell filters was scraped free of cells and the cell number in the lower surface was counted (i.e. the number of labeled cells migrated from the upper to the lower surface). To verify the driving force of migration, MSCs (for the upper chamber) were pre-incubated with 200 ng/mL AMD3100 (a specific SDF-1 antagonist, Sigma) for 30 min at 37°C in some experimental groups. To avoid the possible contribution from materials rather than cells in the lower chamber, data from the wells containing materials but without any replated spheroids were also collected to contrast the effect.

Table 2. The primer sequences used for qRT-PCR analysis.

Genes	Primer sequences	Primer annealing temperature (°C)
Oct4	5'-TGTGGACCTCAGGTTGGACT 3'-CTTCTGCAGGGCTTTCATGT	58
Sox2	5'-ATGTATAACATGATGGAGACGGAGC 3'-TCACATGTGCGACAGGGGCAGTGT	56
Nanog	5'-CATTCTCCTGCCTCAGCCTC 3'-CCCGTCTCTACTAAAAATACAAAA	58
CXCR4	5'-CCGCTTCTACCCCAATGACT 3'-GGCGAAGAAAGCCAGGAT	58
SDF-1	5'-ACAGGCTGGACAGAGGAGAA 3'-GGGCAAGGGCAAGGGGAAGA	60
GAPDH	5'-AATGTGTCCGTCGTGGATCTGA 3'-AGTGTAGCCCAAGATGCCCTTC	56

Calcium adsorption on the surface of each substrate

Substrates were measured for surface bound calcium. Membranes (PVA, CS, and CS-HA) and cut petri dish (all with 1.5 cm diameter) were placed in each well of a 24-well tissue culture plate where 1 mL of DMEM-LG was added.

After incubation at 37°C for 24 h, the medium was collected for analysis of the free calcium remained in the bulk solution. The surface was gently rinsed with PBS. One mL of EDTA solution (5 mM) was added into each well and incubated at 37°C to elute the surface bound calcium. The EDTA solution was again collected after 24 h. A blank well (TCPS) was used as the control. The concentration of calcium in each of the collected solutions was measured by atomic absorption spectrometry (iCE3300; Thermo Scientific).

Western blot analysis of N-cadherin

Samples were heated to 95°C for 5 min in laemmli sample buffer. The total proteins were separated by 12% SDS-PAGE and blotted to polyvinylidene difluoride membranes (Amersham International Plc, Little Chalfont, UK). Western blots were performed using N-cadherin primary antibodies (Cell Signaling Technology, USA) and GAPDH monoclonal antibody (Epitomics, USA) as the internal control. The membranes were blocked with the blocking buffer (Tris-buffered saline, pH 7.6, containing 0.1% Tween 20 and 5% skimmed milk) for 1 h at room temperature and incubated with the primary antibodies by gentle agitation at 4°C overnight. After further washing, horseradish peroxidase (HRP)-conjugated secondary antibodies (Chemicon) were added to the membranes, which were incubated for 1 h at room temperature. Western Chemiluminescent HRP Substrate (Millipore) was finally added and the images were obtained using a chemiluminescence analyzer.

Animal experiments

Male New Zealand white rabbits weighing 3-3.5 kg were used in this study. Animals were anesthetized with Isoflurane (induction: 4.0-5.0%, maintenance: 2.5-3.5%, under oxygen at the flow rate of 400-1200 mL/min). The knee of hind leg was sanitized after the hair was shaved. The skin and ligament above the medial femur were incised parallel to the patella ligament until the joint cavity was exposed. A full-thickness cylindrical defect of 4-mm diameter and 2-mm depth was created on femoral condyle by a stainless steel drill. ADSCs (~1×10^6 cells in 25 μl PBS) of either dispersed single cells or various spheroids (each formed on Petri dish, PVA, CS, and CS-HA membranes) were transplanted into the defect. The total cell number was kept the same for each group. The cell number in spheroids was previously determined by counting single cells from trypsinized spheroids. Experiments were conducted to estimate the cell number for single cell and spheroid cultures in each well (e.g. ~1×10^5 cells for single cell culture and ~8×10^4 cells for spheroid culture after 72 h). Based on this, we can harvest a certain amount of cells using cells from multiple wells and control the cell number to be the same for each type of experiments. To further evaluate the regeneration potential of ADSC spheroids in cartilage tissue engineering, ~1×10^6 dispersed single cells and spheroids from CS and CS-HA were loaded in the macroporous precision scaffolds made of poly(lactide-co-glycolide) (PLGA) by 3D printing[33]. To facilitate the loading, the cell suspension contained HA (3 mg/mL).[32] PLGA scaffolds were coated with chitosan after activation by air plasma generated from an Openair® plasma system (RD1004, Steinhagen, Germany). The plasma source was the compressed filtered/purified dried air (21% oxygen and 79% nitrogen, pressure 2.5 kg/cm^2, temperature 26°C). The air plasma (1000 W) was ejected from a rotating nozzle with 0.5 cm diameter. The scaffolds were placed at a distance of 10 mm from the plasma-ejecting nozzle. The scan speed of the nozzle was 6.4 m/min. The scaffolds were scanned twice, once on the top and once on the bottom, placed immediately in the chitosan solution (5 μL) for 120 min at 37°C, and washed extensively by distilled water.

The ADSC-loaded scaffolds were incubated in the basal medium for 72 h before implantation. After pre-culture in vitro, the scaffolds with ADSC single cells or spheroids from CS and CS-HA were then implanted into the cartilage defects. 15 μL HA solution (3 mg/mL) was added to the defect following the implantation of ADSCs. Surgery was complete after the incision on the ligament and the skin were closed with 5-0 absorbable chromic and 4-0 nylon suture, respectively. Animals were raised with food and water available ad libitum on a 12 h light/dark cycle for one month. After animals were euthanized, the tissue samples obtained from the defect sites were subjected to histological examination.

Histological examination

Samples were washed by PBS, fixed by 3.7% formaldehyde, and decalcified by 10% formic acid for at least one week. Decalcified samples were dehydrated in graded alcohol, cleared by xylene, and embedded in paraffin. The paraffin blocks were cut into 5-μm sections, which were stained with hematoxylin and eosin (HE) or Safranin O (with Fast Green as counterstain). Stained sections were observed by a light microscope and photographed by a digital camera. The photographs were obtained with a constant strength of light source. The density of the red stain as well as the stained area was analyzed and quantified by the LabWorks™ imaging system, which were presented as the intensity (O.D.) and area (mm^2). The photographs were observed and blindly graded by two observers for hyaline matrix formation, cartilage/subchondral bone structure, and cell/tissue morphology using the histological scoring system established by the International Cartilage Repair Society (ICRS)[34]. Higher scores indicate better regeneration of the damaged cartilage.

Statistical analysis

In all studies, similar experiments were performed independently for at least three times. Numerical values were expressed as the mean ± standard deviation. Reproducibility was confirmed for cells from at least three different batches of isolation. Statistical differences among the experimental

groups were determined by analysis of variance followed by ANOVA, where p values <0.05 were considered significantly significant.

Conclusions

This study employed substrate-dependent MSC spheroids to elucidate the role of regeneration capacity of the spheroids for cartilage tissue engineering. The N-cadherin expression and migration capacity of MSC spheroids varied on different substrates, which was probably associated with the amount of surface bound calcium. The CS-HA spheroids expressed more N-adhesion molecules and had greater migration capacities in vitro. The approach was translatable in a rabbit chondral defect model. Transplantation of CS-HA spheroids in a rabbit chondral defect significantly improved the cartilage regeneration, suggesting the advantage of using spheroids derived on CS-HA substrates in repairing the cartilage defect. In this study, the effect of the substrates on the properties of the spheroids was notable and translatable in the animal study, which underscored the importance of selecting a suitable substrate for spheroid formation in tissue engineering.

Notes and references

[a] Institute of Polymer Science and Engineering, National Taiwan University, Taipei, Taiwan
[b] Department of Mechanical Engineering, National Central University, Taoyuan, Taiwan
[#] Both authors contributed equally to this work.
† Electronic Supplementary Information (ESI) available. See DOI: 10.1039/b000000x/

Reference

1 C.S. Potten, M. Loeffler, *Development*, 1990, **110**, 1001-1020.
2 J.K. Fraser, I. Wulur, Z. Alfonso, M.H. Hedrick, *Trends Biotechnol.*, 2006, **24**, 150-154.
3 L. Aust, B. Devlin, S.J. Foster, Y.D. Halvorsen, K. Hicok, T. du Laney, A. Sen, G.D. Willingmyre, J.M. Gimble, *Cytotherapy*, 2004, **6**, 7-14.
4 J.C. Ra, I.S. Shin, S.H. Kim, S.K. Kang, B.C. Kang, H.Y. Lee, Y.J. Kim, J.Y. Jo, E.J. Yoon, H.J. Choi, E. Kwon. *Stem Cell Dev.*., 2011, **20**, 1297-1308.
5 P. Gir, G. Oni. S.A. Brown, A. Mojallal, R.J. Rohrich, *Plast. Reconstr. Surg.*, 2012, **129**, 1277-1290.
6 R.M. Tenney, D.E. Discher, Stem cells, *Curr. Opin. Cell Biol.*, 2009, **21**, 630-635.
7 J.E. Frith, B. Thomson, P.G. Genever, *Tissue Eng Part C-Me*, 2010, **16**, 735-749.
8 L. Bian, M. Guvendiren, R.L. Mauck, J.A. Burdick, *Proc. Natl. Acad. Sci. U. S. A.*, 2013, **110**, 10117-10122.
9 S. Ziane, S. Schlaubitz, S. Miraux, A. Patwa, C. Lalande, I. Bilem, S. Lepreux, B. Rousseau, J.F. Le Meins, L. Latxague, P. Barthelemy, O. Chassande, *Eur. Cells Mater.*, 2012, **23**, 147-160.
10 T.J. Bartosh, J.H. Ylostalo, A. Mohammadipoor, N. Bazhanov, K. Coble, K. Claypool, R.H. Lee, H. Choi, D.J. Prockop, *Proc. Natl. Acad. Sci. U. S. A.*, 2010, **107**, 13724-13729.
11 J.H. Ylostalo, T.J. Bartosh, K. Coble, D.J. Prockop, *Stem Cells*, 2012, **30**, 2283-2296.
12 R.S. Chen, Y.J. Chen, M.H. Chen, T.H. Young, *J. Biomed. Mater. Res. Part A*, 2007, **83A** , 241-248.
13 K. Hayashi, Y. Tabata, *Acta Biomater.*, 2011, **7**, 2797-2803.
14 G. Su, Y. Zhao, J. Wei, J. Han, L. Chen, Z. Xiao, B. Chen, J. Dai, *Biomaterials*, 2013, **34**, 3215-3222.
15 G.S. Huang, L.G. Dai, B.L. Yen, S.H. Hsu, *Biomaterials*, 2011, **32,** 6929-6945.
16 B. Johnstone, T.M. Hering, A.I. Caplan, V.M. Goldberg, J.U. Yoo, *Exp. Cell Res.*, 1998, **238**, 265-272.
17 C.H. Chang, H.Y. Lin, H.W. Fang, S.T. Loo, S.C. Hung, Y.C. Ho, C.C. Chen, F.H. Lin, H.C. Liu, *Artif. Organs*, 2008, **32**, 561-566.
18 S.H. Hsu, G.S. Huang, S.Y. Lin, F. Feng, T.T. Ho, Y.C. Liao, *Tissue Eng. Part A*, 2012, **18**, 67-79.
19 J.I. Lee, M. Sato, H.W. Kim, J. Mochida, *Eur. Cells Mater.*, 2011, **22**, 275-290.
20 S. Suzuki, T. Muneta, K. Tsuji, S. Ichinose, H. Makino, A. Umezawa, I. Sekiya, *Arthritis Res. Ther.*, 2012, **14**, R136.
21 L. Quintana, N.I. zur Nieden, C.E. Semino, *Tissue Eng. Part B Rev.*, 2009, **15**, 29-41.
22 S.H. Hsu, G.S. Huang, F. Feng, *Biomaterials*, 2012, **33**, 2642-2655.
23 B.R. Son, L.A. Marquez-Curtis, M. Kucia, M. Wysoczynski, A.R. Turner, J. Ratajczak, M.Z. Ratajczak, A. Janowska-Wieczorek, *Stem Cells*, 2006, **24**, 1254-1264.
24 D. Kuraitis, P. Zhang, Y. Zhang, D.T. Padavan, K. McEwan, T. Sofrenovic, D. McKee, J. Zhang, M. Griffith, X. Cao, A. Musaro, M. Ruel, E.J. Suuronen, *Eur. Cells Mater.*, 2011, **22**, 109-123.
25 L.G. Guang, A.L. Boskey, W. Zhu, *Int. J. Biochem. Cell Biol.*, 2012, **44**, 1825-1833.
26 A. Mendelson, E. Frank, C. Allred, E. Jones, M. Chen, W. Zhao, J.J. Mao, *FASEB J.*, 2011, **25**, 3496-3504.
27 A. Sukegawa, N. Iwasaki, Y. Kasahara, T. Onodera, T. Igarashi, A. Minami, *Tissue Eng. Part A.*, 2012, **18**, 934-945.
28 T.T. Lau, D.A. Wang, *Expert Opin. Biol. Ther.*, 2011, **11**, 189-197.
29 H.Y. Yeh, B.H. Liu S.H. Hsu, *Biomaterials*, 2012, **33**, 8943-8954.
30 S.H. Hsu, Y.H. Ni, Y.C. Lee, *Macromol. Biosci.*, 2013, **13**, 1100-1109.
31 H. Katagiri, T. Muneta, K. Tsuji, M. Horie, H. Koga, N. Ozeki, E. Kobayashi, I. Sekiya, *Biochem. Biophys. Res. Commun.*, 2013, **435**, 603-609.
32 G.S. Huang, C.S.Tseng, B.L. Yen, L.G. Dai, P.S. Hsieh, S.H. Hsu, Eur. Cell. Mater., 2013, **26**,179-194.
33 H.J. Yen, S.H. Hsu, C.S. Tseng, J.P. Huang, C.L. Tsai, *Tissue Eng. Part A.*, 2009, **15**, 965-975.
34 P. Mainil-Varlet, T. Aigner, M. Brittberg, P. Bullough, A. Hollander, E. Hunziker, R. Kandel, S. Nehrer, K. Pritzker, S. Roberts, E. Stauffer, *J. Bone Joint Surg.- Am.*, 2003, **85**, 45-57.

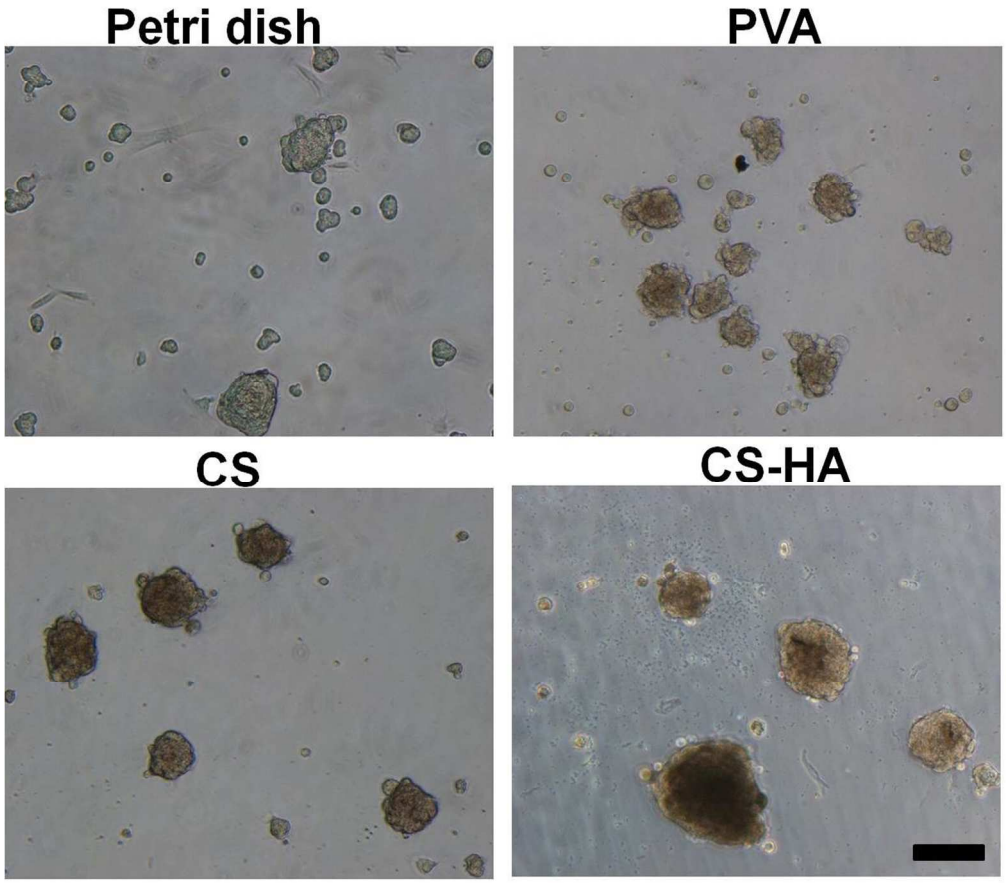

184x166mm (300 x 300 DPI)

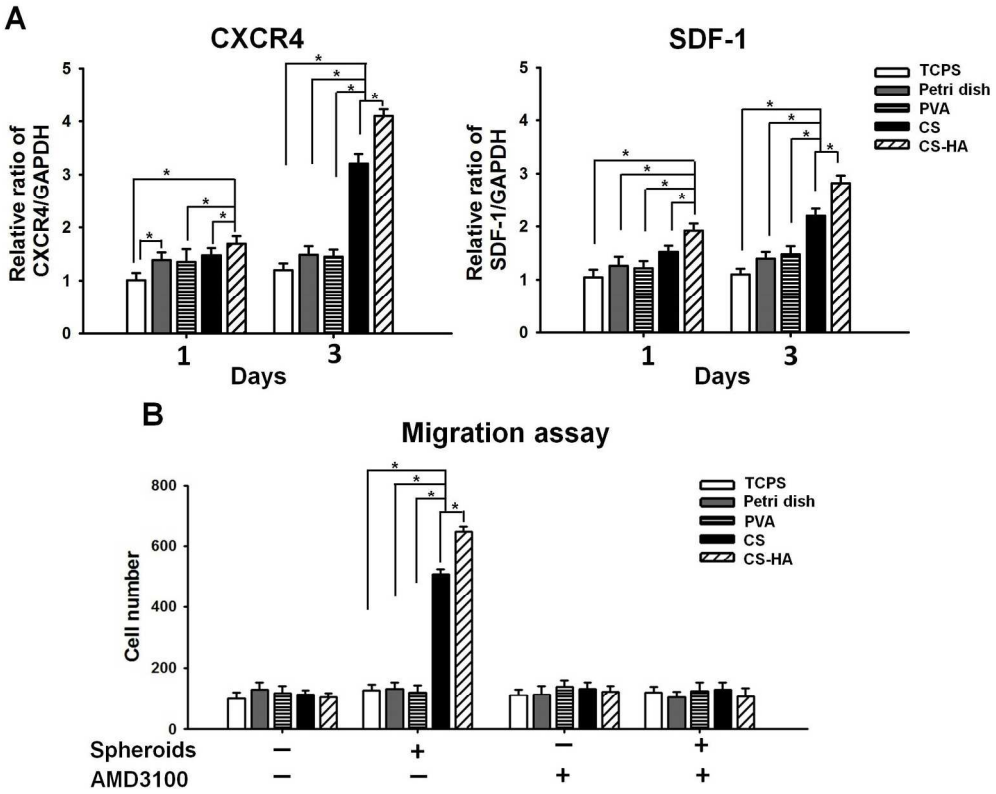

283x225mm (300 x 300 DPI)

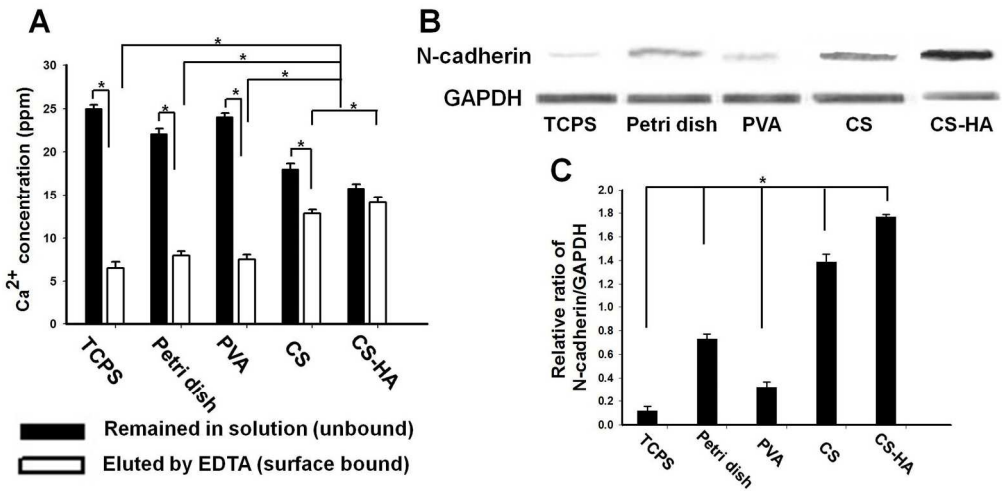

222x108mm (300 x 300 DPI)

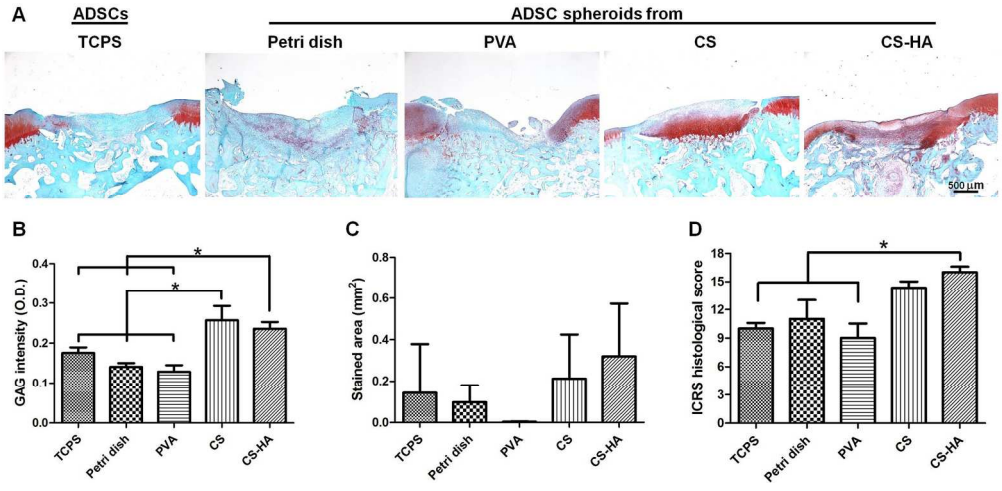

204x97mm (300 x 300 DPI)

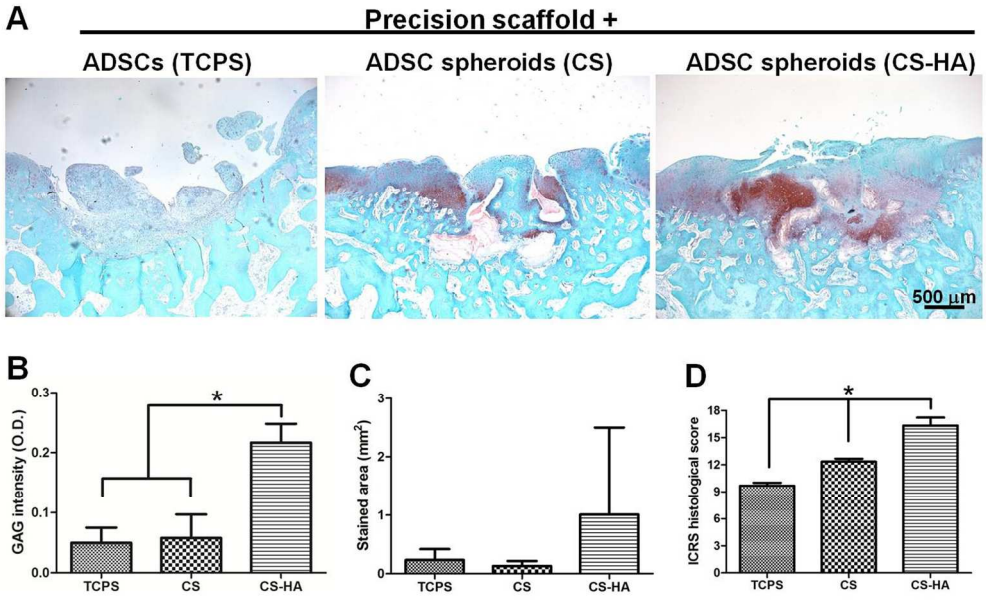

160x97mm (300 x 300 DPI)

Table of Contents

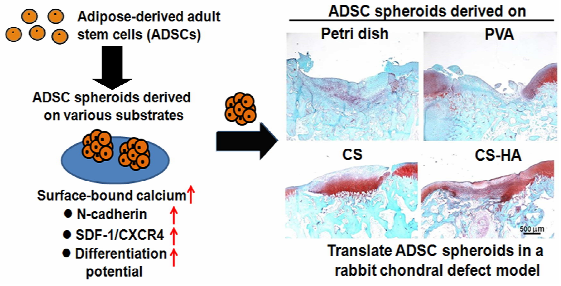

ADSC spheroids derived on various biomaterials present different in vitro properties, which may explain the different efficacies in cartilage repair.